OPTIMAL SENSOR-TARGET GEOMETRIES FOR DOPPLER-SHIFT TARGET LOCALIZATION

Ngoc Hung Nguyen[*] *and Kutluyıl Doğançay*[†*]

[*]Institute for Telecommunications Research, [†]School of Engineering
University of South Australia, Mawson Lakes SA 5095, Australia

ABSTRACT

Doppler-shift target localization has recently attracted renewed interest due to its wide range of applications. In this paper we analyze the optimal sensor-target geometries for the Doppler-shift target localization problem where the position and velocity of a moving target are estimated from Doppler-shift measurements taken at stationary sensors. The analysis is based on minimizing the estimation uncertainty, which is equivalent to maximizing the determinant of the Fisher information matrix. In particular, the optimal geometries that maximize the estimation accuracy for target position only, velocity only, and both position and velocity, are investigated. The analytical findings are verified by numerical examples.

Index Terms— Optimal sensor placement, Doppler-shift measurement, localization, Fisher information matrix

1. INTRODUCTION

Position and velocity estimation of a moving object using Doppler-shift measurements has a long history [1, 2]. Recently this problem has attracted renewed interest due to its wide-ranging applications in radar, sonar, passive surveillance, wireless sensor networks, acoustic source localization, and satellite positioning and navigation [3–7]. Existing literature mainly focuses on examining the observability of a Doppler-shift sensor system [6, 7], and developing target localization and tracking algorithms for different applications [3–5]. In contrast, far less research attention has been given to the performance of Doppler-shift target localization. Among different factors such as measurement error, number of sensors, and transmitted wavelength, the sensor-target geometry plays a very important role in determining the performance of Doppler-shift target localization [7].

Focusing on the sensor-target geometry, numerical experiments were carried out in [8] to evaluate the localization performance of moving submarine targets with four and six fixed Doppler-shift sensors under different sensor geometries. Simulation results on the geometric dilution of precision (GDOP) for bi/multi-static Doppler-shift radar were reported in [7]. Recently, the optimal sensor placement for the Doppler-shift target localization problem of a stationary target using Doppler-shift measurements from multiple moving sensor platforms has been derived in [9], where the optimal angular separation between the sensors was shown to depend on the noise levels and the angular velocities of the sensors, and to be mathematically equivalent to the optimal angular separation problem for angle-of-arrival (AOA) localization in [10].

In this paper, we analyze the optimal sensor-target geometries for the Doppler-shift target localization problem in which the position and velocity of a moving target are estimated using the Doppler-shift measurements obtained from a number of stationary sensors. We adopt the minimization of the area of the estimation confidence region, which is equivalent to maximizing the determinant of the Fisher information matrix (FIM), as the optimality criterion for sensor-target geometries. This criterion, commonly known as the D-optimality criterion [11], has been widely used to derive the optimal sensor placement for different target localization problems [9–13].

Depending upon applications, one may aim to optimize the accuracy in position estimate only, velocity estimate only, or both position and velocity estimates. In this paper, we derive the optimal geometries for position estimate only. Our analysis shows that more than one optimal solution exists. An optimal solution is obtained when the sensor bearing angles have the absolute value of $\pi/3$ rad with a sign sequence $b_i \in \{1, -1\}$ minimizing $\left(\sum b_i/w_i\right)^2$, where b_i is the sign of the bearing angle of the ith sensor and w_i is a positive constant associated with the noise level and the sensor-target range of the ith sensor. Other optimal solutions can be generated from this optimal solution by reflecting one or more sensors about the target position. The optimal angular geometries for velocity estimate are more straightforward than those for position estimate because the FIM component corresponding to velocity estimate is mathematically equivalent to the FIM for AOA localization in [10] and range-based localization in [12]. This equivalence has been reported in [6]. A preliminary result on the optimal angular geometry for both position and velocity estimates is also provided for the case of equal noise variances and equal sensor-target distances with the number of sensors being a multiple of four. The paper concludes with numerical examples to corroborate the analytical findings.

978-0-9928626-3-3/15/$31.00 ©2015 IEEE

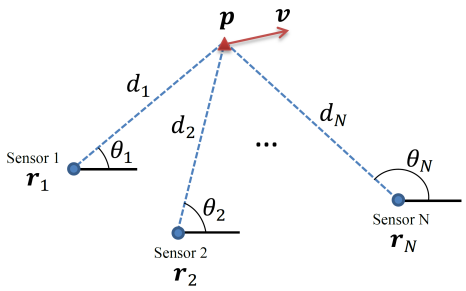

Fig. 1. Estimation of position and velocity of a moving target using N stationary Doppler-shift sensors.

2. PROBLEM STATEMENT

Consider a Doppler-shift target localization problem in the 2D-plane where the position and velocity of a moving target are estimated using the Doppler-shift measurements obtained from N stationary sensors. The localization problem is depicted in Fig. 1, in which $\mathbf{p} = [p_x, p_y]^T$ and $\mathbf{v} = [v_x, v_y]^T$ are the unknown target position and velocity, respectively, with the superscript T denoting matrix transpose, and $\mathbf{r}_i = [x_i, y_i]^T$ is the position of the ith sensor with $i = 1, \ldots, N$. The Doppler-shift measurement at the ith sensor is given by

$$\tilde{f}_i = f_i + e_i,\ f_i = f_{c,i}\frac{2\,\dot{d}_i}{c} = \frac{2\,f_{c,i}}{c}\frac{(\mathbf{p}-\mathbf{r}_i)^T\mathbf{v}}{d_i}. \quad (1)$$

Here $f_{c,i}$ is the carrier frequency of the transmitted signal at the ith sensor, $d_i = \|\mathbf{p} - \mathbf{r}_i\|$ is the distance between the target and the ith sensor, c is the speed of signal propagation, and e_i is the zero-mean independent Gaussian noise error at the ith sensor. Note that the error covariance $E\{e_i^2\}$ is usually dependent on the target-sensor distances among other things.

Normalizing f_i by the factor of $2\,f_{c,i}/c$, the Doppler-shift measurement at the ith sensor becomes

$$\tilde{z}_i = z_i + n_i \text{ with } z_i = \frac{(\mathbf{p}-\mathbf{r}_i)^T\mathbf{v}}{d_i} \quad (2)$$

where n_i is the measurement error with $E\{n_i^2\} = \sigma_i^2$ (i.e., $E\{e_i^2\} = 4\,f_{c,i}^2\sigma_i^2/c^2$). Writing the Doppler shift measurement (2) in vector form gives

$$\tilde{\mathbf{z}} = \mathbf{z} + \mathbf{n} = [z_1, \ldots, z_N]^T + [n_1, \ldots, n_N]^T \quad (3)$$

with the error covariance matrix of $\mathbf{\Sigma} = E\{\mathbf{n}\mathbf{n}^T\} = \text{diag}(\sigma_1^2, \ldots, \sigma_N^2)$.

Solving (3) for $\mathbf{x} = [\mathbf{p}^T\ \mathbf{v}^T]^T$ in the least-squares sense requires at least four Doppler-shift measurements (i.e., $N \geq 4$). However, more than one solution (ghost target) exists for $N = 4$ and hence prior information about the region where the target lies and the velocity range of the target is required [6]. Therefore, at least five Doppler-shift measurements (i.e., $N \geq 5$) are needed to provide a unique solution for the unknown $\mathbf{x}$.

With the independent Gaussian noise error for Doppler-shift measurements, the FIM for the considered Doppler-shift target localization problem is given by

$$\mathbf{\Phi} = \mathbf{J}_0^T\mathbf{\Sigma}^{-1}\mathbf{J}_0 \quad (4)$$

where $\mathbf{J}_0 = [\mathbf{u}_1, \ldots, \mathbf{u}_N]^T$ is the Jacobian matrix of $\mathbf{z}$ in (3) evaluated at the true value of $\mathbf{x}$ with

$$\mathbf{u}_i = \begin{bmatrix} \frac{1}{d_i}(v_x \sin^2\theta_i - v_y \sin\theta_i\cos\theta_i) \\ \frac{1}{d_i}(v_y \cos^2\theta_i - v_x \sin\theta_i\cos\theta_i) \\ \cos\theta_i \\ \sin\theta_i \end{bmatrix}. \quad (5)$$

Here, θ_i denotes the bearing angle of the ith sensor as illustrated in Fig. 1.

Without any loss of generality, we rotate the coordinate system so that $v_x = V$ and $v_y = 0$, where V is the target speed. Consequently, the FIM becomes

$$\mathbf{\Phi} = \sum_{i=1}^{N}\frac{1}{\sigma_i^2}\mathbf{u}_i\mathbf{u}_i^T = \begin{bmatrix} \mathbf{\Phi_{pp}} & \mathbf{\Phi_{pv}} \\ \mathbf{\Phi}_{\mathbf{pv}}^T & \mathbf{\Phi_{vv}} \end{bmatrix} \quad (6)$$

where

$$\mathbf{\Phi_{pp}} = \sum_{i=1}^{N}\frac{V^2}{\sigma_i^2 d_i^2}\begin{bmatrix} \sin^4\theta_i & -\sin^3\theta_i\cos\theta_i \\ -\sin^3\theta_i\cos\theta_i & \sin^2\theta_i\cos^2\theta_i \end{bmatrix}$$

$$\mathbf{\Phi_{vv}} = \sum_{i=1}^{N}\frac{1}{\sigma_i^2}\begin{bmatrix} \cos^2\theta_i & \sin\theta_i\cos\theta_i \\ \sin\theta_i\cos\theta_i & \sin^2\theta_i \end{bmatrix}$$

$$\mathbf{\Phi_{pv}} = \sum_{i=1}^{N}\frac{V}{\sigma_i^2 d_i}\begin{bmatrix} \sin^2\theta_i\cos\theta_i & \sin^3\theta_i \\ -\sin\theta_i\cos^2\theta_i & -\sin^2\theta_i\cos\theta_i \end{bmatrix}. \quad (7)$$

In practice, the true target velocity is not available, but it can be approximated by an estimate obtained from sensor measurements.

In this paper, we aim to derive the optimal sensor-target geometries for Doppler-shift target localization by minimizing the area of the estimation confidence region. For an efficient unbiased estimator, the area of 1-σ error ellipse, i.e., the 39.4% confidence region is inversely proportional to the determinant of the FIM matrix [14]. Thus, minimizing the area of the estimation confidence region is equivalent to maximizing the determinant of FIM. As a result, the optimization problem is now defined as

$$\{\theta_1^*, \ldots, \theta_N^*\} = \underset{\{\theta_1,\ldots,\theta_N\}}{\arg\max}\ |\mathfrak{F}| \quad (8)$$

where $|\cdot|$ denotes matrix determinant and $\mathfrak{F}$ is $\mathbf{\Phi_{pp}}$ (the FIM component corresponding to position estimate), $\mathbf{\Phi_{vv}}$ (the FIM component corresponding to velocity estimate), or the complete FIM matrix $\mathbf{\Phi}$ depending upon the optimization objective. It is noted that the Doppler-shift localization

algorithm under consideration is assumed to be nearly efficient and unbiased so that the estimation error covariance can be approximated by its Cramér-Rao lower bound (CRLB), i.e., the inverse of FIM, and the FIM in (6) can be used to characterize the estimation performance.

3. OPTIMAL GEOMETRY ANALYSIS

3.1. Optimal angular geometries for position estimate

To optimize the accuracy in position estimate, we aim to maximize the determinant of $\mathbf{\Phi_{pp}}$ which is the FIM component corresponding to position estimate. From (7), the determinant of $\mathbf{\Phi_{pp}}$ is given by

$$|\mathbf{\Phi_{pp}}| = V^4 \left\{ \sum_{i=1}^{N} \frac{\sin^4\theta_i}{\sigma_i^2 d_i^2} \sum_{i=1}^{N} \frac{\sin^2\theta_i \cos^2\theta_i}{\sigma_i^2 d_i^2} - \left(\sum_{i=1}^{N} \frac{\sin^3\theta_i \cos\theta_i}{\sigma_i^2 d_i^2} \right)^2 \right\}. \quad (9)$$

To reveal the similarity between $|\mathbf{\Phi_{pp}}|$ and the determinant of FIM for multistatic time-of-arrival localization with a single transmitter and multiple receivers in [15], we let $\alpha_i = 2\theta_i$ and substitute $\theta_i = \alpha_i/2$ into (9), which yields

$$|\mathbf{\Phi_{pp}}| = \frac{V^4}{16} \left\{ \sum_{i=1}^{N} \frac{(1-\cos\alpha_i)^2}{\sigma_i^2 d_i^2} \sum_{i=1}^{N} \frac{\sin^2\alpha_i}{\sigma_i^2 d_i^2} - \left(\sum_{i=1}^{N} \frac{(1-\cos\alpha_i)\sin\alpha_i}{\sigma_i^2 d_i^2} \right)^2 \right\}. \quad (10)$$

Let $\beta_i = \pi - \alpha_i$ (i.e., $\cos\alpha_i = \cos(\pi-\beta_i) = -\cos\beta_i$ and $\sin\alpha_i = \sin(\pi-\beta_i) = \sin\beta_i$). Then $|\mathbf{\Phi_{pp}}|$ becomes

$$|\mathbf{\Phi_{pp}}| = \frac{V^4}{16} \left\{ \sum_{i=1}^{N} \frac{(1+\cos\beta_i)^2}{\sigma_i^2 d_i^2} \sum_{i=1}^{N} \frac{\sin^2\beta_i}{\sigma_i^2 d_i^2} - \left(\sum_{i=1}^{N} \frac{(1+\cos\beta_i)\sin\beta_i}{\sigma_i^2 d_i^2} \right)^2 \right\}. \quad (11)$$

To find the optimal angular geometry, $|\mathbf{\Phi_{pp}}|$ is maximized with respect to $\beta_1, \ldots, \beta_N$ for given values of $\sigma_1, \ldots, \sigma_N$, $d_1, \ldots, d_N$. The optimal values of $\theta_1, \ldots, \theta_N$ then follow from $\theta_i = (\pi - \beta_i)/2$. Note that the optimal angular geometry for position estimate does not depend on the target speed V.

The solution for maximizing (11) in terms of $\beta_1, \ldots, \beta_N$ is given as follows [15]. For given values of $\sigma_1, \ldots, \sigma_N$, $d_1, \ldots, d_N$, $|\mathbf{\Phi_{pp}}|$ is maximized at

$$|\mathbf{\Phi_{pp}}|_{\max} = \frac{27\,V^2}{256} \left[\left(\sum_{i=1}^{N} \frac{1}{\sigma_i^2 d_i^2} \right)^2 - \left(\sum_{i=1}^{N} \frac{b_i^*}{\sigma_i^2 d_i^2} \right)^2 \right] \quad (12)$$

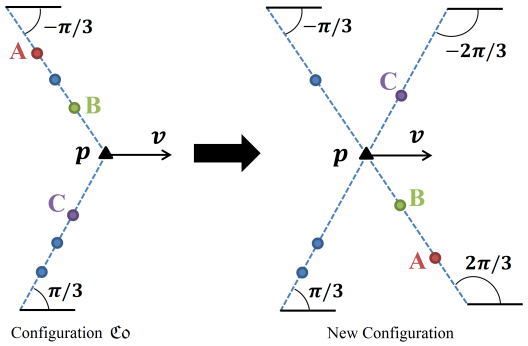

Fig. 2. An example of generating new optimal configurations from initial optimal configuration $\mathfrak{Eo}$ for position estimates. Here sensors **A**, **B** and **C** are reflected about target.

when $|\beta_i^*| = \pi/3$ for all $i = 1, \ldots, N$ and $b_i^* = \text{sgn}(\beta_i^*)$ satisfies

$$\{b_1^*, \ldots, b_N^*\} = \underset{b_i \in \{1,-1\}, 1 \le i \le N}{\arg\min} \left(\sum_{i=1}^{N} \frac{b_i}{\sigma_i^2 d_i^2} \right)^2 \quad (13)$$

with $\text{sgn}(\cdot)$ denoting the *signum* function.

The optimal bearing angles $\theta_1^*, \ldots, \theta_N^*$ are given by:

- If $\beta_i^* = \pi/3$, then $\theta_i^* = \pi/3$ or $-2\pi/3$.
- If $\beta_i^* = -\pi/3$, then $\theta_i^* = -\pi/3$ or $2\pi/3$.

It is apparent from β_i^* to θ_i^* transformations that more than one optimal angular geometry exists. All the optimal angular sensor-target configurations can be found by the following approach:

1. Find the initial optimal configuration, referred to as configuration $\mathfrak{Eo}$, by setting $|\theta_i^*| = \pi/3$ for all $i = 1, \ldots, N$, and $\text{sgn}(\theta_i^*) = b_i^*$ according to (13).
2. Other optimal configurations are obtained by moving one or more sensors from $\mathbf{r}_i$ to $2\mathbf{p} - \mathbf{r}_i$, i.e., reflecting one or more sensors about the target as illustrated in Fig. 2.

3.2. Optimal angular geometries for velocity estimate

Referring to (7), the determinant of $\mathbf{\Phi_{vv}}$, the FIM component corresponding to velocity estimate, is given by

$$|\mathbf{\Phi_{vv}}| = \frac{1}{4} \left\{ \left(\sum_{i=1}^{N} \frac{1}{\sigma_i^2} \right)^2 - \left(\sum_{i=1}^{N} \frac{\sin 2\theta_i}{\sigma_i^2} \right)^2 - \left(\sum_{i=1}^{N} \frac{\cos 2\theta_i}{\sigma_i^2} \right)^2 \right\} \quad (14)$$

which is mathematically equivalent to the determinant of the FIM for AOA localization [10] and range-based localization [12]. The solution for maximizing (14) with respect to $\theta_1, \ldots, \theta_N$ can be found in [10].

3.3. Preliminary results on optimal geometries for both position and velocity estimates

The optimal angular geometries for position estimate and for velocity estimate obtained in sections 3.1 and 3.2 are different. In many applications, the estimation accuracies in both target position and velocity are required to be optimal. This can be achieved by maximizing the determinant of $\mathbf{\Phi}$ in (6). However, $\mathbf{\Phi}$ is a 4×4 matrix and hence deriving a closed-form solution for maximizing $|\mathbf{\Phi}|$ is a very challenging task.

Optimal geometries produce diagonally dominant, or where possible, diagonal FIMs. In what follows we propose a method for finding the optimal geometry for $N = 4k$ ($k = 1, 2, \dots$) with $\sigma_1 = \cdots = \sigma_N = \sigma$ and $d_1 = \cdots = d_N = d$.

As $\mathbf{\Phi}$ is a symmetric positive semi-definite matrix, i.e, $\mathbf{\Phi} \geq \mathbf{0}$, the following Hadamard's inequality holds [16]

$$|\mathbf{\Phi}| \leq \phi_{11}\phi_{22}\phi_{33}\phi_{44} \tag{15}$$

where $\phi_{11}, \dots, \phi_{44}$ are the diagonal elements of $\mathbf{\Phi}$. The equality in (15) holds if and only if $\mathbf{\Phi}$ is diagonal. Using (7) and (15), we obtain

$$|\mathbf{\Phi}| \leq \frac{V^4}{\sigma^8 d^4} \sum_{i=1}^{N} a_i^2 \sum_{i=1}^{N} a_i(1-a_i) \sum_{i=1}^{N} (1-a_i) \sum_{i=1}^{N} a_i \tag{16}$$

where $a_i = \sin^2\theta_i$. Applying the arithmetic and harmonic means inequality [17], we have

$$|\mathbf{\Phi}| \leq \frac{V^4}{4\sigma^8 d^4} \left(\sum_{i=1}^{N} a_i^2 \sum_{i=1}^{N} (1-a_i) + \sum_{i=1}^{N} a_i(1-a_i) \sum_{i=1}^{N} a_i \right)^2 \tag{17}$$

with equality if and only if $\sum_{i=1}^{N} a_i^2 \sum_{i=1}^{N}(1-a_i) = \sum_{i=1}^{N} a_i(1-a_i) \sum_{i=1}^{N} a_i$ which is achieved when $N\sum_{i=1}^{N} a_i^2 = \left(\sum_{i=1}^{N} a_i\right)^2$. Based on the power mean inequality [17], this can only be achieved when $a_1 = \cdots = a_N$.

To maximize the term inside the square operation of (17)

$$f = N\sum_{i=1}^{N} a_i^2 - 2\sum_{i=1}^{N} a_i^2 \sum_{i=1}^{N} a_i + \left(\sum_{i=1}^{N} a_i\right)^2 \tag{18}$$

we set

$$\frac{\partial f}{\partial a_i} = 2\left\{ \left(N - 2\sum_{i=1}^{N} a_i \right) a_i + \left(\sum_{i=1}^{N} a_i - \sum_{i=1}^{N} a_i^2 \right) \right\} = 0. \tag{19}$$

Noting that $N - 2\sum_{i=1}^{N} a_i = 0$ and $\sum_{i=1}^{N} a_i - \sum_{i=1}^{N} a_i^2 = 0$ cannot hold at once because it requires $\sum_{i=1}^{N} a_i = \sum_{i=1}^{N} a_i^2 = N/2$ which cannot be satisfied as $0 \leq a_i \leq 1$, (19) is satisfied for all $i = 1, \dots, N$ if

$$a_1 = \cdots = a_N = \frac{\sum_{i=1}^{N} a_i - \sum_{i=1}^{N} a_i^2}{N - 2\sum_{i=1}^{N} a_i}. \tag{20}$$

Hence f has two critical points:

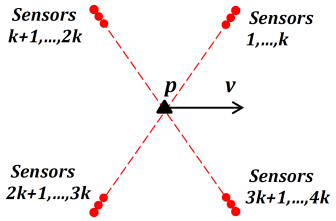

Fig. 3. Optimal geometry for both position and velocity estimate.

- Minimum point: $a_1 = \cdots = a_N = 0$ with $f = 0$.
- Maximum point: $a_1 = \cdots = a_N = 2/3$ with $f = \frac{8N^2}{27}$.

From the above analysis, we can see that $\sin^2\theta_i = 2/3$ for all $i = 1, \dots, N$ will satisfy the equality conditions of (16) and (17) as well as maximizing f in (18). To satisfy the equality condition of (15) (i.e., $\mathbf{\Phi}$ is diagonal), the number of sensors is required to be a multiple of four ($N = 4k$ with $k = 1, 2, \dots$). Thus, the optimal geometry is given by

$$\theta_i = \begin{cases} \arcsin(2/3) - 180^\circ = -125.26^\circ, \ i = 1, \dots, k \\ -\arcsin(2/3) = -54.74^\circ, \ i = k+1, \dots, 2k \\ \arcsin(2/3) = 54.74^\circ, \ i = 2k+1, \dots, 3k \\ 180^\circ - \arcsin(2/3) = 125.26^\circ, \ i = 3k+1, \dots, 4k \end{cases}$$

which is illustrated in Fig. 3. The resulting value of determinant of FIM is $|\mathbf{\Phi}|_{\max} = \left(\frac{4N^2V^2}{27\sigma^4d^2}\right)^2$. Note that, in contrast to the optimal geometries for position only and velocity only in section 3.1 and 3.2, reflecting the sensors about the target will change $\mathbf{\Phi}$ and hence affect the optimality of the sensor-target geometry for both position and velocity estimates.

Deriving the optimal geometry for $N \neq 4k$ is more challenging as $\mathbf{\Phi}$ cannot be made diagonal for $\sin^2\theta_1 = \cdots = \sin^2\theta_N = 2/3$. This will be considered in our future work.

4. NUMERICAL EXAMPLES

In this section we verify the analytical findings for the optimal angular geometries by way of numerical examples. To numerically find the optimal global maxima of determinant of FIM, we employ the genetic algorithm [18]. The genetic algorithm is halted if the average relative change in the best fitness function value over 50 consecutive generations is less than or equal to 10^{-15} for Table 1 and 2, and 10^{-30} for Table 3, or if the number of iterations reaches the limit of 5000.

Tables 1 and 2 report the numerical solutions of the optimal geometries for position estimate, averaged over 6000 runs, after eliminating the wrong solutions and transforming all the remaining solutions back into configuration $\mathfrak{C}_\circ$, for different noise variances and target-sensor ranges with $N = 4$ and 5, respectively. By comparing the numerical solutions in Tables 1 and 2 and the analytical results of configuration $\mathfrak{C}_\circ$ derived in section 3.1, we observe a perfect agreement between the simulation and analytical results.

	θ_1	θ_2	θ_3	θ_4
Case 1[a]	60.00°	60.00°	-60.00°	-60.00°
Case 2[b]	60.00°	60.00°	60.00°	-60.00°
Case 3[c]	60.00°	-60.00°	-60.00°	60.00°

[a] $w_1 = \cdots = w_4 = 1$ with $w_i = \sigma_i^2 d_i^2$ (the permutations of the sensors are allowed).
[b] $w_1 = 1, w_2 = 1/2, w_3 = 1/3, w_4 = 1/6$.
[c] $w_1 = 1, w_2 = 1/2, w_3 = 1/3, w_4 = 1/4$.

Table 1. Genetic algorithm solutions for $N = 4$.

	θ_1	θ_2	θ_3	θ_4	θ_5
Case 1[a]	60.00°	60.00°	60.00°	-60.00°	-60.00°
Case 2[b]	60.00°	60.00°	60.00°	60.00°	-60.00°
Case 3[c]	60.00°	-60.00°	-60.00°	-60.00°	60.00°

[a] $w_1 = \cdots = w_5 = 1$ with $w_i = \sigma_i^2 d_i^2$ (the permutations of the sensors are allowed).
[b] $w_1 = 1, w_2 = 1/2, w_3 = 1/3, w_4 = 1/4, w_5 = 1/10$.
[c] $w_1 = 1, w_2 = 1/2, w_3 = 1/3, w_4 = 1/4, w_5 = 1/8$.

Table 2. Genetic algorithm solutions for $N = 5$.

θ_1	θ_2	θ_3	θ_4
-125.26°	-54.74°	54.74°	125.26°

Note: the permutations of the sensors are allowed.

Table 3. Genetic algorithm solution of optimal geometry for both position and velocity estimates.

Table 3 shows the numerical solution of the optimal geometry for both position and velocity estimates, averaged over 6000 runs, for $\sigma_1 = \cdots = \sigma_N = 1$ m/s, $d_1 = \cdots = d_N = 1$ km and $V = 50$ m/s with $N = 4$. We observe that the numerical solution in Table 3 exhibits a perfect match with the analytical result derived in section 3.3.

5. CONCLUSION

This paper has investigated the optimal sensor-target geometries for Doppler-only target localization based on maximizing the determinant of FIM. Our analysis showed that the optimal geometries for position estimate are not unique as the FIM for position estimate is invariant to sensors being reflected about the target. Therefore, from an initial optimal configuration $\mathfrak{Co}$, a multitude of optimal configurations can be generated simply by reflecting one or more sensors about the target. The optimal angular geometry for velocity estimate is mathematically equivalent to the optimal angular geometry problem for AOA localization in [10] and range-based localization in [12]. A preliminary result was also provided on the challenging problem of finding an optimal geometry for both position and velocity estimates. The analytical findings of the paper were demonstrated via numerical examples.

REFERENCES

[1] E. J. Barlow, "Doppler radar," *Proc. IRE*, vol. 37, no. 4, pp. 340–355, Apr. 1949.

[2] Y. T. Chan and F. L. Jardine, "Target localization and tracking from Doppler-shift measurements," *IEEE J. Ocean. Eng.*, vol. 15, no. 3, pp. 251–257, July 1990.

[3] B. Ristic and A. Farina, "Target tracking via multi-static Doppler shifts," *IET Radar, Sonar Navigation*, vol. 7, no. 5, pp. 508–516, June 2013.

[4] A. Amar and A. J. Weiss, "Localization of narrowband radio emitters based on Doppler frequency shifts," *IEEE Trans. Signal Process.*, vol. 56, no. 11, pp. 5500–5508, Nov. 2008.

[5] D. Lindgren, G. Hendeby, and F. Gustafsson, "Distributed localization using acoustic Doppler," *Signal Process.*, vol. 107, no. 0, pp. 43–53, 2015.

[6] I. Shames, A. N. Bishop, M. Smith, and B. D. O. Anderson, "Doppler shift target localization," *IEEE Trans. Aerosp. Electron. Syst.*, vol. 49, no. 1, pp. 266–276, Jan. 2013.

[7] Y. Xiao, P. Wei, and T. Yuan, "Observability and performance analysis of bi/multi-static Doppler-only radar," *IEEE Trans. Aerosp. Electron. Syst.*, vol. 46, no. 4, pp. 1654–1667, Oct. 2010.

[8] I. Levesque and J. Bondaryk, "Performance issues concerning Doppler-only localization of submarine targets," Tech. Rep., DTIC Document, 2000.

[9] N. H. Nguyen and K. Dogancay, "Optimal sensor placement for Doppler shift target localization," in *Proc. IEEE Int. Radar Conf.*, 2015, pp. 1677–1682.

[10] K. Dogancay and H. Hmam, "Optimal angular sensor separation for AOA localization," *Signal Process.*, vol. 88, no. 5, pp. 1248–1260, 2008.

[11] D. Ucinski, *Optimal Measurement Methods for Distributed Parameter System Identification*, CRC Press, Boca Raton, 2004.

[12] A. N. Bishop, B. Fidan, B. D. O. Anderson, K. Dogancay, and P. N. Pathirana, "Optimality analysis of sensor-target localization geometries," *Automatica*, vol. 46, no. 3, pp. 479–492, 2010.

[13] N. H. Nguyen and K. Dogancay, "Optimal geometry analysis for elliptic target localization by multistatic radar with independent bistatic channels," in *Proc. IEEE Int. Conf. Acoust., Speech, Signal Process.*, 2015, pp. 2764–2768.

[14] Y. Oshman and P. Davidson, "Optimization of observer trajectories for bearings-only target localization," *IEEE Trans. Aerosp. Electron. Syst.*, vol. 35, no. 3, pp. 892–902, July 1999.

[15] N. H. Nguyen and K. Dogancay, "Optimal geometry analysis for multistatic TOA localization," *IEEE Trans. Signal Process.*, under review.

[16] R. A. Horn and C. R. Johnson, *Matrix Analysis*, Cambridge University Press, New York, 1985.

[17] P. S. Bullen, *Handbook of Means and Their Inequalities*, Springer, Netherlands, Dordrecht, 2003.

[18] D. E. Goldberg, *Genetic Algorithms in Search, Optimization, and Machine Learning*, Addison-Wesley, 1989.